Supporting Information

New p-type Al-substituted $SrSnO_3$ perovskite for TCO applications?

Leila Ben Amor,[a b] Besma Belgacem,[a] Jean-Sébastien Filhol,[b] Marie-Liesse Doublet,[b] Mouna Ben Yahia* [b] and Rached Ben Hassen [a]

Experimental section:

Synthesis of $SrSnO_3:Al^{3+}$

The polycrystalline phases of $SrSn_{1-x}Al_xO_3$ (x=0, 0.20 and 0.50) were synthesized by a high temperature solid-state reaction process. Typically, stoichiometric amounts of Al_2O_3 (99.99%), SnO_2 (99.99%) and $SrCO_3$ (99.99%) starting materials were used as precursors. Initially, $SrCO_3$ was calcined to decompose carbonate at 1273 K for 12 hours before weighing, then these precursors were weighted and mixed thoroughly in an agate mortar using ethanol as a grinding media. The starting material mixture was first calcined at 1173 K in an alumina crucible and annealed at 1473 and 1573 K for 12 h to obtain desired solid solutions.

Materials characterization

The X-ray diffraction (XRD) analysis data was collected in the 2θ range between 10 and 90° using a high-resolution powder diffractometer 'PANalyticalX'pert' in Bragg-Brentano geometry (θ-2θ) with Cu radiation (λKα = 1.54056 Å). And the microscopic morphology and elemental analysis of the synthesized samples were investigated via scanning electron microscope (SEM-FEI Quanta 200 FEG), which was equipped with the energy dispersive X-ray spectroscopy (EDX). The optical measurements of all the compounds were performed at room temperature by UV-Visible-Near Infrared Spectrophotometer (JASCO V-770 UV-Vis/NIR) in the wavelength range of 190-2700 nm.

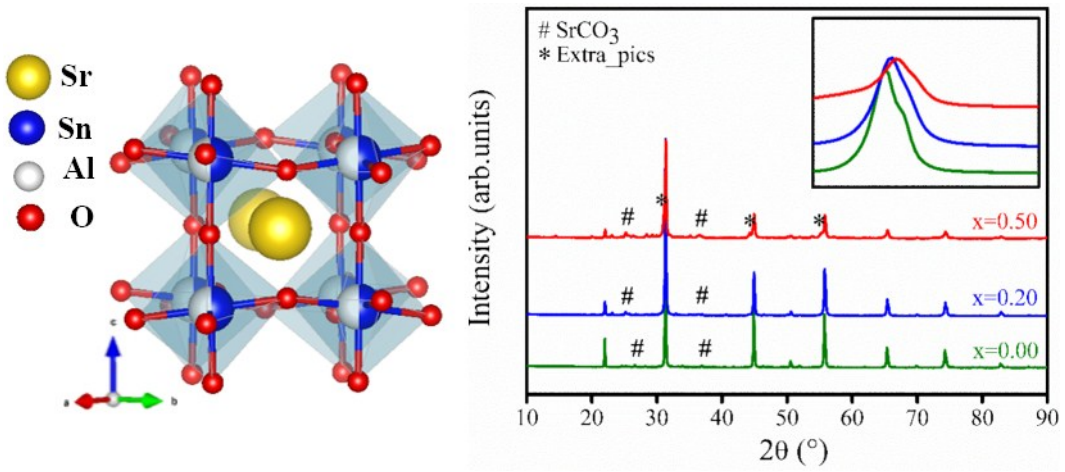

Fig S1: $SrSn_xAl_{1-x}O_3$ structure, X-ray diffraction patterns and enlargement at 2θ ~ 31° of SrSn1-xAlxO3 (x=0, 0.20 and 0.50)

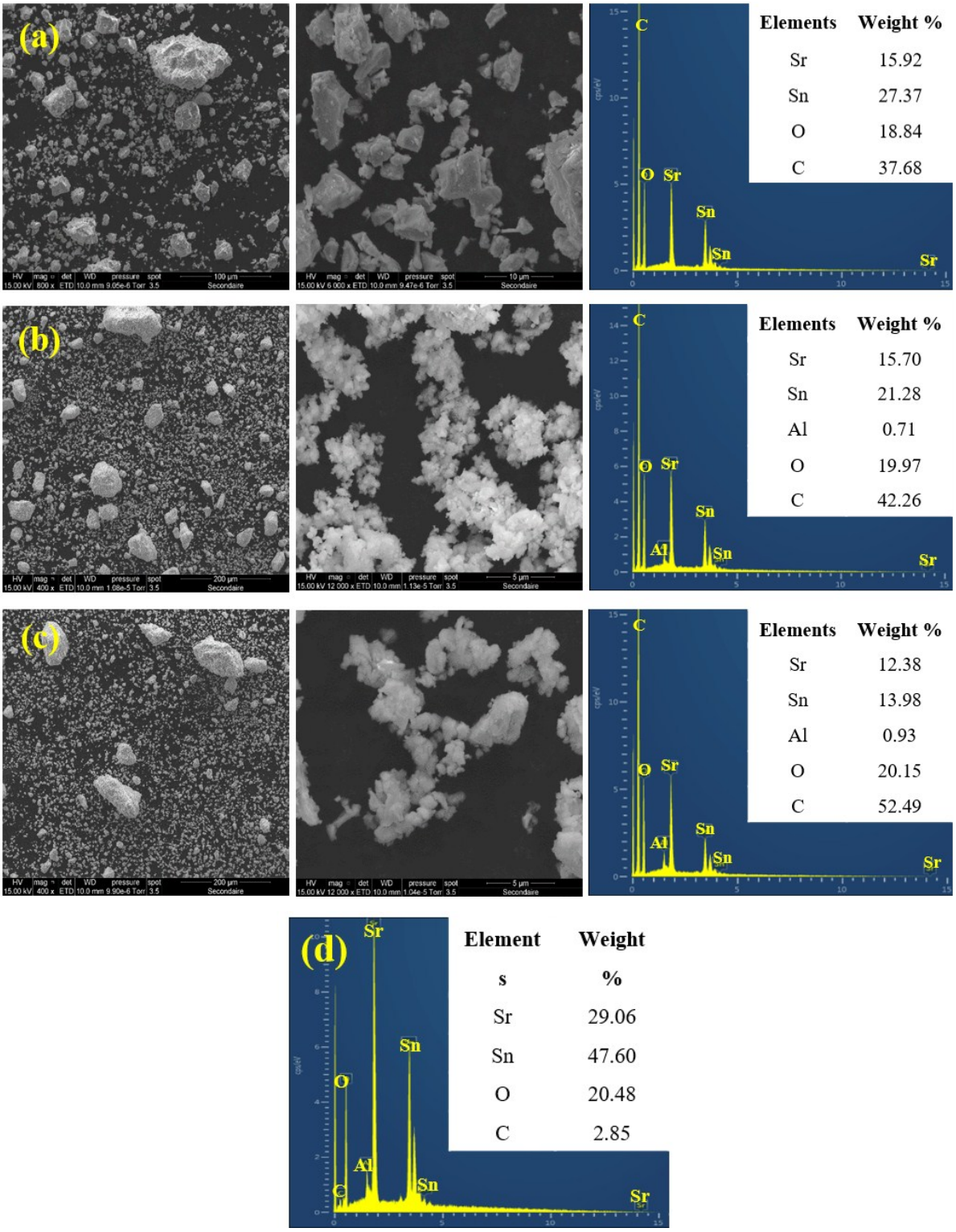

Fig S2: SEM and EDX analysis of (a) $SrSnO_3$, (b) $SrSn_{0.8}Al_{0.2}O_3$ (c) $SrSn_{0.5}Al_{0.5}O_3$. (d) EDX spectra of $SrSn_{0.5}Al_{0.5}O_3$ when pellet is used

Goldschmidt and distortion octahedral factors

For all compositions, the Goldschmidt tolerance (t) and distortion octahedral (μ) factors remain in the range [0.8-1.1] and [0.41-0.73], respectively. They correspond to t=0.96, 0.975, 0.997 and μ=0.49, 0.47, 0.44 for x = 0, 0.2 and 0.5, respectively, which confirms the phases stability.

Tauc's formula

Optical band-gaps (E_g^{opt}) are determined using Tauc's theory of optical absorption for semiconductors by means of $\alpha h\nu = B(h\nu - E_g^{opt})^{1/2}$ formula, where E_g^{opt} is the Tauc optical band gap, α=2303*A/d (A=optical density and d = sample thickness), hν is incident photon energy. $(\alpha h\nu)^2$ versus (hν) are then plotted for different xAl_{Sn} compositions. The extrapolation of the straight-line portion of $(\alpha h\nu)^2$ *plots at* $\alpha = 0$ *give an estimation of* E_g^{opt}.

Theoretical calculations:

First-principles Density Functional Theory (DFT) calculations were performed using all-electron atomic basis sets and the B3LYP functional for exchange and correlation potential, as implemented in CRYSTAL17.[1–4] Gaussian basis set of 976633-111G*, 97654-1G*, 86-21G* and 8-411G* were employed to describe the Sn, Sr, Al and O atoms. A sampling of 150 points within the irreducible Brillouin zone is used. All atom coordinates and lattice parameters were fully relaxed using conjugate gradient energy minimization and the force tolerance for structural relaxation was set to 2.10^{-5} eV/Å. A structural model with a theoretical composition of xAl_{Sn}=0.25 was constructed to mimic the experimental composition of xAl_{Sn}=0.2.

Thermodynamic calculations are performed using 2×1×2 supercell using Vienna Ab inito software plane wave code (VASP).[5–7] Due to calculation cost induced by the use of hybrid function, the generalized gradient approximation PBEsol functional was preferred coupled to the use of projected augmented wave pseudopotentials (PAW).[8,9] A plane waves cut-off energy of 600 eV had been applied.

Basin Hopping procedure:

Basin hoping optimization technique was used to map the potential energy surface (SEP) at different xAl_{Sn} compositions. Starting from a given structure, it allows constructing new one by deforming the initial cell parameters and randomly moving and/or permuting atoms. This step is followed by an energy minimization procedure to obtain a new structure (new local minimum) from which a new guess can be formed again. This method increases the chance to discover new minima in the SEP, for a given composition.[10]

The relative energy of the orthorhombic and new cubic structure as a function of xAl_{Sn} composition is depicted on figure S3.

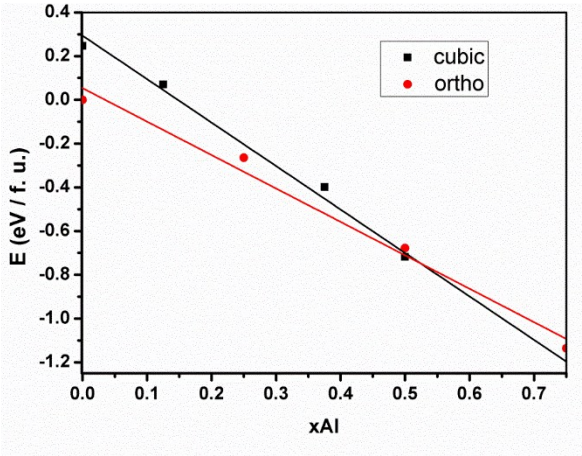

Fig. S3: Relative stability of orthorhombic versus cubic phase depending on the Al_{Sn} ratio

Formation energy of defects:

The O_2 free energy is known to be badly reproduced in DFT. To properly evaluate this contribution, a correction of +0,87 eV was applied to the calculated formation energy of O_2. This correction was extracted from the comparison of calculated and experimental formation enthalpies of several oxides SiO_2, GeO_2, Al_2O_3, Ga_20_3, SrO, SnO_2, In_2O_3 and SeO_2 using PBEsol functional. Our obtained correction, are equal to the one published by Mellan and coworkers.[11]

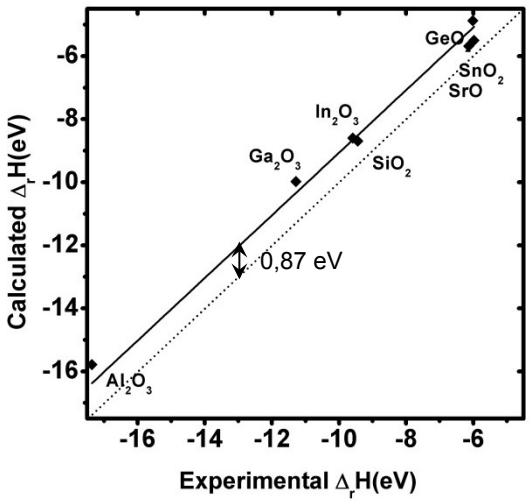

Fig. S4: Experimental formation enthalpy of a serial of oxide compounds as a function of the theoretical formation enthalpy. Deviation from the slope y = x allows to evaluate the correction to apply to O_2 energy.

The formation enthalpy of CO_2 was considered without including correction. The free energies of both molecules are then obtained by adding the TS term at 300K. The results of the different free energy formation of V_{Sr} at different composition using the following reaction $SrSn_{1-x}Al_xO_3 + (\frac{y}{2})O_2 + yCO_2 \rightarrow Sr_{1-y}Sn_{1-x}Al_xO_3 + ySrCO_3$ (1) are summarized on Table 1. Note that the entropies of condensed phase are neglected.

Table. S1: Free energy formation of V_{Sr}= y = 0,0625 defects following reaction (1)

x	$\Delta_r G$ (meV)
0	-162
0,0625	-170
0.125	-171
0,25	-191
0,375	-174
0,5	-164

Fukui function:

Fukui function is defined as the change of the electronic density with regards to an external perturbation, herein the modification of the number of electron at constant external potential. $f(r) = \frac{\partial \rho(r)}{\partial N}$ which is normalized, is a useful tool for probing reactivity and the nature of frontier-electron.[12] The Fukui function depicted for SSO correspond to the $f^-(r) = \left[\frac{\partial \rho(r)}{\partial N}\right]^-$, when N increases from N_0-δ to N_0 and N_0= number of valence electron of SSO. Accordingly, f^- mimic the highest occupied states. $f^+(r) = \left[\frac{\partial \rho(r)}{\partial N}\right]^+$ when N increases from N'_0 to $N'_0+\delta$ (N'_0 = *number of valence electron of SSAO)* was used to illustrate the lowest unoccupied states of SSAO.

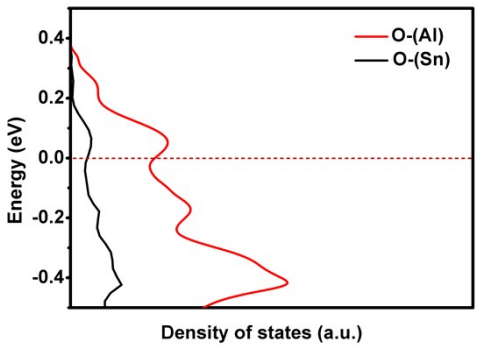

Fig. S5: Projected density of states on O connected to Al and Sn.

Calculations of band structure are performed on conventional cell and the used critical points are illustrated on Figure S6.

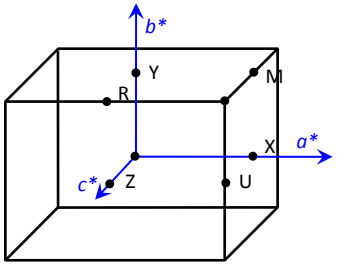

Fig. S6: Irreducible first Brillouin zone of Pnma structure.

1 A. D. Becke, *J. Chem. Phys.*, 1993, **98**, 1372–1377.
2 C. Lee, W. Yang and R. G. Parr, *Phys. Rev. B*, 1988, **37**, 785–789.
3 A. Erba, J. Baima, I. Bush, R. Orlando and R. Dovesi, *J. Chem. Theory Comput.*, 2017, **13**, 5019–5027.
4 R. Dovesi, A. Erba, R. Orlando, C. M. Zicovich-Wilson, B. Civalleri, L. Maschio, M. Rérat, S. Casassa, J. Baima, S. Salustro and B. Kirtman, *Wiley Interdisciplinary Reviews: Computational Molecular Science*, 2018, **8**, e1360.
5 G. Kresse and J. Furthmüller, *Computational Materials Science*, 1996, **6**, 15–50.
6 G. Kresse and J. Hafner, *Physical Review B*, 558.
7 G. Kresse and J. Furthmüller, *Physical review B*, 1996, **54**, 11169.
8 G. I. Csonka, J. P. Perdew, A. Ruzsinszky, P. H. T. Philipsen, S. Lebègue, J. Paier, O. A. Vydrov and J. G. Ángyán, *Phys. Rev. B*, 2009, **79**, 155107.
9 G. Kresse and D. Joubert, *Phys. Rev. B*, 1999, **59**, 1758–1775.
10 D. J. Wales and J. P. K. Doye, *J. Phys. Chem. A*, 1997, **101**, 5111–5116.
11 T. A. Mellan, K. P. Maenetja, P. E. Ngoepe, S. M. Woodley, C. R. A. Catlow and R. Grau-Crespo, *Journal of Materials Chemistry A*, 2013, **1**, 14879.
12 R. G. Parr and W. Yang, *J. Am. Chem. Soc.*, 1984, **106**, 4049–4050.